Electroabsorption Spectroscopic Studies of Dipolar Ruthenium(II) Complexes Possessing Large Quadratic Nonlinear Optical Responses

Benjamin J. Coe,*,† James A. Harris,† and Bruce S. Brunschwig*,‡

Department of Chemistry, University of Manchester, Oxford Road, Manchester M13 9PL, U.K., and Chemistry Department, Brookhaven National Laboratory, P.O. Box 5000, Upton, New York 11973-5000

Received: June 19, 2001; In Final Form: November 5, 2001

A series of 20 ruthenium(II) complex salts, known to exhibit large molecular static first hyperpolarizabilities β_0[HRS] from hyper-Rayleigh scattering measurements on acetonitrile solutions at 298 K (Coe, B. J.; et al. *Inorg. Chem*. **1997**, *36*, 3284; **1998**, *37*, 3391; *J. Chem. Soc., Dalton Trans*. **1999**, 3617), have been studied by using electroabsorption spectroscopy in butyronitrile glasses at 77 K. The salts are of the form *trans*-$[Ru^{II}(NH_3)_4(L^D)(L^A)][PF_6]_3$ [L^D = NH_3 and L^A = *N*-methyl-4,4′-bipyridinium (MeQ^+) (**1**), *N*-phenyl-4,4′-bipyridinium (PhQ^+) (**2**), *N*-(4-acetylphenyl)-4,4′-bipyridinium (4-$AcPhQ^+$) (**3**), *N*-(2,4-dinitrophenyl)-4,4′-bipyridinium (2,4-$DNPhQ^+$) (**4**), *N*-methyl-4-[*trans*-2-(4-pyridyl)ethenyl]pyridinium ($Mebpe^+$) (**5**), *N*-phenyl-4-[*trans*-2-(4-pyridyl)ethenyl]pyridinium ($Phbpe^+$) (**6**), or *N*-methyl-2,7-diazapyrenium ($Medap^+$) (**7**); L^D = 1-methylimidazole and L^A = MeQ^+ (**8**), PhQ^+ (**9**), 4-$AcPhQ^+$ (**10**), *N*-(2-pyrimidyl)-4,4′-bipyridinium (2-$PymQ^+$) (**11**), $Mebpe^+$ (**12**), or $Phbpe^+$ (**13**); L^D = 4-(dimethylamino)pyridine and L^A = MeQ^+ (**14**), PhQ^+ (**15**) or 4-$AcPhQ^+$ (**16**); L^D = pyridine and L^A = 2-$PymQ^+$ (**17**), $Mebpe^+$ (**18**) or $Phbpe^+$ (**19**); L^D = 4-(dimethylamino)benzonitrile and L^A = MeQ^+ (**20**)]. The electroabsorption spectra afford dipole moment changes $\Delta\mu_{12}$ for the visible metal-to-ligand charge-transfer (MLCT) excitations of the dipolar complexes. The transition dipole moments μ_{12} cover a range of ca. 4−7 D and generally increase with the electron accepting strength of L^A, most notably on replacing an *N*-methyl with a *N*-phenyl substituent. The $\Delta\mu_{12}$ values are large (ca. 14−21 D) and generally increase with the size of L^A. Comparison of experimental and calculated diabatic dipole moment changes $\Delta\mu_{ab}$ suggests that the orbital(s) that receive the MLCT electron are delocalized only over the first two aryl rings. ZINDO calculations on the pentaammine complexes do not accurately reproduce the MLCT energies or β_0[HRS] values, but they can predict the dipole properties with reasonable accuracy and also indicate that the low lying π^* orbitals span only the first two rings of L^A. β_0[Stark] values of **1**−**20** calculated according to the two-state model by using $\beta_0 = 3\Delta\mu(\mu_{12})^2/(E_{max})^2$ (E_{max} = MLCT energy maximum) are mostly in good agreement with β_0[HRS]. The β_0[Stark] values are the first meaningful first hyperpolarizabilities for **18** and **20**. The electroabsorption results confirm the unusually large magnitudes of β_0 in **1**−**20** and also that *N*-arylation enhances β_0, the latter effect being most significant in the 4,4′-bipyridinium-based complexes. Increases in β_0 are generally associated with decreases in E_{max} and increases in both μ_{12} and $\Delta\mu_{12}$, and insertion of a *trans*-CH=CH bridge into the 4,4′-bipyridinium unit of L^A enhances β_0 by ca. 35−50%.

Introduction

The search for new molecular materials possessing nonlinear optical (NLO) properties, as candidates for applications in optoelectronic and photonic devices, continues to gather momentum.[1] Within this field, an increasing amount of attention has recently been paid to organotransition metal complexes which offer possibilities for combination of NLO effects with other molecular electronic properties.[2] We are currently investigating the quadratic (second-order) NLO behavior of ruthenium ammine complexes, the redox and spectroscopic properties of which have been thoroughly characterized over the years.[3] Our studies, involving hyper-Rayleigh scattering (HRS) measurements,[4] have shown that Ru^{II} penta- and tetraammines can display very large β_0 (static first hyperpolarizability) values which are associated with intense, low energy metal-to-ligand charge-transfer (MLCT) absorptions.[5] The MLCT and NLO properties of these chromophores show a high degree of tunability and are also redox-switchable.[6]

Of the various spectroscopic techniques which have been used to study Ru ammines, electroabsorption (Stark) spectroscopy[7] is among the more recently to be exploited. This technique has been applied to mono- and binuclear $\{Ru^{II}(NH_3)_5\}^{2+}$ complexes of pyrazine or 4,4′-bipyridine[8] and also to a wide variety of other mononuclear $\{Ru^{II}(NH_3)_5\}^{2+}$ and $\{Ru^{III}(NH_3)_5\}^{3+}$ complexes.[9] We are interested in using electroabsorption spectroscopy as a tool to improve our understanding of the observed large molecular quadratic NLO responses in Ru^{II} ammines.[5] Of particular relevance to the present report are very recent electroabsorption studies involving cyanide-bridged $\{Ru^{III}(NH_3)_n\}^{3+}$ (n = 4 or 5) mixed-valence complexes[10] and the tris-chelate $[Ru^{II}$(*trans*-4,4′-diethylaminostyryl-2,2′-bipyridine)$_3]^{2+}$ which exhibit pronounced quadratic NLO properties.[11] Other NLO-active organic molecules such as donor−acceptor poly-

* To whom correspondence should be addressed. E-mail: b.coe@man.ac.uk. E-mail: brunschwig@bnl.gov.
† University of Manchester.
‡ Brookhaven National Laboratory.

10.1021/jp012320q CCC: $22.00
Published on Web 01/17/2002

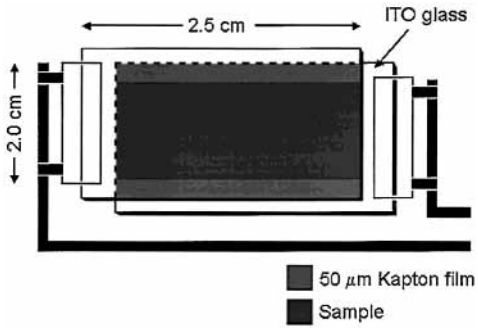

Figure 1. Sample cell assembly for the electroabsorption experiments.

enes,[12] porphyrins,[13] and metallocenyl derivatives[14] have also been investigated by using electroabsorption measurements. A small number of the results contained within this article have been previously communicated.[15]

Experimental Section

Materials. All of the complex salts were synthesized according to previously published procedures.[5a,c,d] The identity and purity of the samples used for electroabsorption studies were confirmed by using ^{1}H NMR spectroscopy and elemental analyses.

Instrumentation and Measurements. The electroabsorption apparatus and experimental procedures were as previously reported,[9b] but incorporated the minor modifications described below. Butyronitrile (Aldrich) was used as the glassing medium. The electroabsorption spectrum for each complex was measured a minimum of three times using different field strengths. The electroabsorption signal was always found to be quadratic in the field, and the fit parameters presented are the average values.

Sample Cell. Two strips of Kapton film (50 μm, Dupont) were arranged so that they lay flush with the two long edges of the ITO glass (Figure 1). The cell was held vertically, and a drop of sample was placed onto the top horizontal edge of the lower plate where it could run into the cavity produced by the Kapton film spacers.

Glass Characterization. Absorption spectra on the sample cell taken in the near-IR region (800−1700 nm at 298 K) show oscillations that are due to the interference between the light reflected from the two glass surfaces that are 50 μm apart. The absorbance data were analyzed as follows: a smoothed baseline was subtracted from the data, the Fourier transform (FT) of these data was then obtained, and the power spectrum was calculated. The maximum in the power spectrum was then taken as the product of the refractive index with the cell spacing, $n \times d$. The FT analysis of the oscillations on cells charged with air ($n_1 = 1.00$) and butyronitrile ($n_1 = 1.38$) at room temperature and 77 K allowed the determination of the distance between the electrodes (52.2 μm) and the refractive index of the frozen samples. The measured density of butyronitrile between 298 and 193 K was linear with temperature, and the density is estimated to be 15% higher at 77 K than at 298 K. A static dielectric constant D_s of the glass of 4.01 was determined from capacitance measurements made with a BK Precision 878 capacitance meter at 1 kHz. The method was calibrated with nine materials of known dielectric constant.

Data Treatment. The data analysis was carried out as previously described,[9b] by using the first and second derivatives of the absorption spectrum for analysis of the electroabsorption $\Delta\epsilon(\nu)$ spectrum in terms of the Liptay treatment:[16]

$$\Delta\epsilon(\nu)/\nu = \left[A_x\epsilon(\nu)/\nu + \frac{B_x}{15h}\frac{\partial(\epsilon(\nu)/\nu)}{\partial\nu} + \frac{C_x}{30h^2}\frac{\partial^2(\epsilon(\nu)/\nu)}{\partial\nu^2}\right]F_{int}^{\ 2} \quad (1)$$

where ν is the frequency of the light in Hz. For a randomly oriented, fixed sample, the following relationships hold:

$$A_x = A_1 + (3\cos^2(\chi) - 1)A_2 \quad (2)$$

$$B_x = B_1 + (3\cos^2(\chi) - 1)B_2 \quad (3)$$

$$C_x = C_1 + (3\cos^2(\chi) - 1)C_2 \quad (4)$$

where χ is the angle between the direction of the applied electric field and the polarization direction of the incident light. The dipole moment change for the MLCT excitation is obtained from the coefficient of the second derivative term:

$$|\Delta\mu_{12}| = \sqrt{C_1/5} \quad (5)$$

$$|\mathrm{m}\cdot\Delta\mu_{12}| = \sqrt{C_2/3 + C_1/15} \quad (6)$$

where m is the unit transition dipole moment, $\mu_{12}/|\mu_{12}|$. The internal electric field is related to the applied external field by $F_{int} = f_{int}F_{ext}$. For the butyronitrile medium used here, the local field correction f_{int} is estimated as 1.33.[9b]

A two-state model (ground and excited) can be used to analyze the charge-transfer transitions. If ψ_a and ψ_b denote the wave functions of the zero-order diabatic states (i.e., the metal-centered and ligand-centered localized states), then their interaction gives two adiabatic wave functions $\psi_1 = c_a\psi_a + c_b\psi_b$ (ground) and $\psi_2 = c_a\psi_b - c_b\psi_a$ (excited), where the overlap integral is neglected and the mixing coefficients are normalized. This model gives

$$\Delta\mu_{ab}^{\ 2} = \Delta\mu_{12}^{\ 2} + 4\mu_{12}^{\ 2} \quad (7)$$

where $\Delta\mu_{ab}$ is the dipole moment difference between the diabatic states, $\Delta\mu_{12}$ is the observed (adiabatic) dipole moment difference, and μ_{12} is the transition dipole moment. The latter can be determined from the oscillator strength f_{os} of the transition by

$$|\mu_{12}| = [f_{os}/(1.08 \times 10^{-5}(E_{max}))]^{1/2} \quad (8)$$

where E_{max} is the energy of the MLCT maximum (in wavenumbers). The degree of delocalization $c_b^{\ 2}$ and electronic coupling matrix element H_{ab} for the diabatic states are given by

$$c_b^{\ 2} = \frac{1}{2}\left[1 - \left(\frac{\Delta\mu_{12}^{\ 2}}{\Delta\mu_{12}^{\ 2} + 4(\mu_{12})^2}\right)^{1/2}\right] \quad (9)$$

$$|H_{ab}| = \left|\frac{E_{max}\mu_{12}}{\Delta\mu_{ab}}\right| \quad (10)$$

If the polarizability change $\Delta\alpha$ and hyperpolarizability β_0 tensors have only nonzero elements along the direction of the charge-transfer, then these quantities are given by

$$\Delta\alpha = -4\frac{(\mu_{12})^2}{E_{max}} \quad (11)$$

$$\beta_0 = \frac{3\Delta\mu_{12}(\mu_{12})^2}{(E_{max})^2} \quad (12)$$

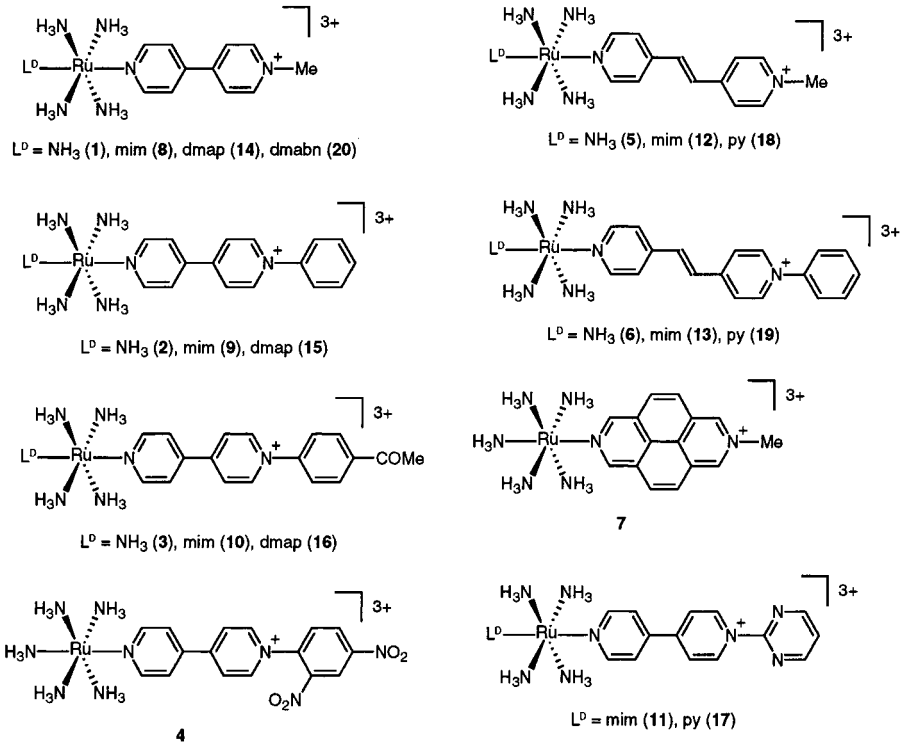

Figure 2. Structures of the complex cations in the salts **1**−**20** [mim = 1-methylimidazole; dmap = 4-(dimethylamino)pyridine; py = pyridine; dmabn = 4-(dimethylamino)benzonitrile].

Calculations. All semiempirical and molecular mechanics calculations were carried out by using MSI Cerius^2 software.[17] The molecules were constructed and their structures optimized using the Cerius^2 universal force field.[18] After optimization of the unsolvated complex, the Ru−N(L^A) distance was adjusted to 1.97 Å. Approximately 25 water molecules were then added around the ammine end of the complex, and the water structure was optimized while holding the structure of the complex fixed using a Dreiding force field.[19] To obtain reasonable hydrogen bonding distances, the charge on the complex was increased to +4 or +5, and equilibrated over the molecule. ZINDO calculations were then performed on these structures. To determine the change in the polarization of the ligand L^A in the MLCT excited-state, ZINDO calculations were performed on the free ligand L^A with a dummy atom placed 2 Å from the coordinating atom. The calculations were performed using a charge on the dummy atom that varied between 0 and 4. The position of the center of charge was obtained from the Mulliken charges on each atom. In almost all cases, a plot of this position against the charge on the dummy atom gave a straight line, and the change in position that was due to a unit charge change was determined from the slope. This value was used to estimate the increase in the polarization of the diabatic excited state of the complex.

Results and Discussion

Electroabsorption Studies. The structures of the complexes in the salts **1**−**20** are shown in Figure 2. As found previously with related Ru^{II} ammine complexes,[9b] the electroabsorption spectra of **1**−**20** were successfully modeled in terms of a large second derivative term, a small first derivative component, and a negligible zeroth derivative contribution. Spectra were also recorded for five other salts, *trans*-[Ru^{II}(NH$_3$)$_4$(L^D)(L^A)][PF$_6$]$_3$ [L^D = NH$_3$ and L^A = 2-PymQ$^+$;[5d] L^D = mim and L^A = Medap$^+$;[5d] L^D = py and L^A = Medap$^+$;[5d] and L^D = dmabn and L^A = PhQ$^+$ or 4-AcPhQ$^+$],[5c] but satisfactory data fits could not be obtained. Representative absorption spectra, electroabsorption spectra, and the spectral components for the salts **2**, **10**, and **16** are presented in Figure 3. Parameters derived from fitting the electroabsorption spectra to Liptay's equations[15] are given in Table 1, together with the oscillator strengths f_{os}, MLCT absorption maxima λ_{max} at 298 and 77 K, and the values inferred from eqs 5 and 6 for $|\Delta\mu_{12}|$ and $|\mathbf{m}\cdot\Delta\mu_{12}|$ in multiples of f_{int}. Deviations are of the order of 10^{-58} C^{2}m^2 (5−10%), 10^{-38} Cm^2 V^{-1} (ca. 50%), and ca. 10^{-20} m^2 V^{-2} for the second, first, and zeroth derivative terms, respectively. The $f_{int}|\Delta\mu_{12}|$ values cover a range of 16−28 D which includes those found previously for [Ru^{II}(NH$_3$)$_5$(L^A)]Cl$_3$ (L^A = *N*-protonated 4,4′-bipyridine) (20 and 23.1 D).[8b,9b] In almost all cases, $f_{int}|\Delta\mu_{12}|$ and $f_{int}|\mathbf{m}\cdot\Delta\mu_{12}|$ agree within experimental error, confirming that the transition dipole moment and the dipole moment change lie along the same axis.

As observed previously,[9b] in all cases, the MLCT bands undergo marked red-shifts in the 77 K glass. The changes in E_{max} are larger for the Mebpe$^+$/Phbpe$^+$ complexes than for the MeQ$^+$/PhQ$^+$ complexes [the average shifts in eV (L^A) are −0.13 (MeQ$^+$), −0.22 (Mebpe$^+$), −0.15 (PhQ$^+$), −0.21 (Phbpe$^+$)]. The f_{os} values were determined directly by numerical integration of the digitized absorption spectra and do not differ significantly (±5%) from those obtained by using the band maxima and half widths and assuming Gaussian absorption profiles. Although the band maxima and half widths change between 298 and 77 K, the f_{os} values show very little temperature dependence (≤5%).

The dipole moment changes $\Delta\mu_{12}$ and the transition dipole moments μ_{12} for MLCT excitation are of direct relevance to the quadratic molecular NLO responses of salts **1**−**20**. In all cases, both $\Delta\mu_{12}$ and μ_{12} lie along the Ru-L^A bond. Values of these quantities, calculated from the electroabsorption results in Table 1 by using f_{int} = 1.33 and eqs 7 and 8, are given in Table 2. Also included in Table 2 are the nominal metal-to-center-of-ligand distances r^0 (obtained from measurements on the Cerius^2 models) and $\Delta\mu_{ab}$ (diabatic dipole moment change),

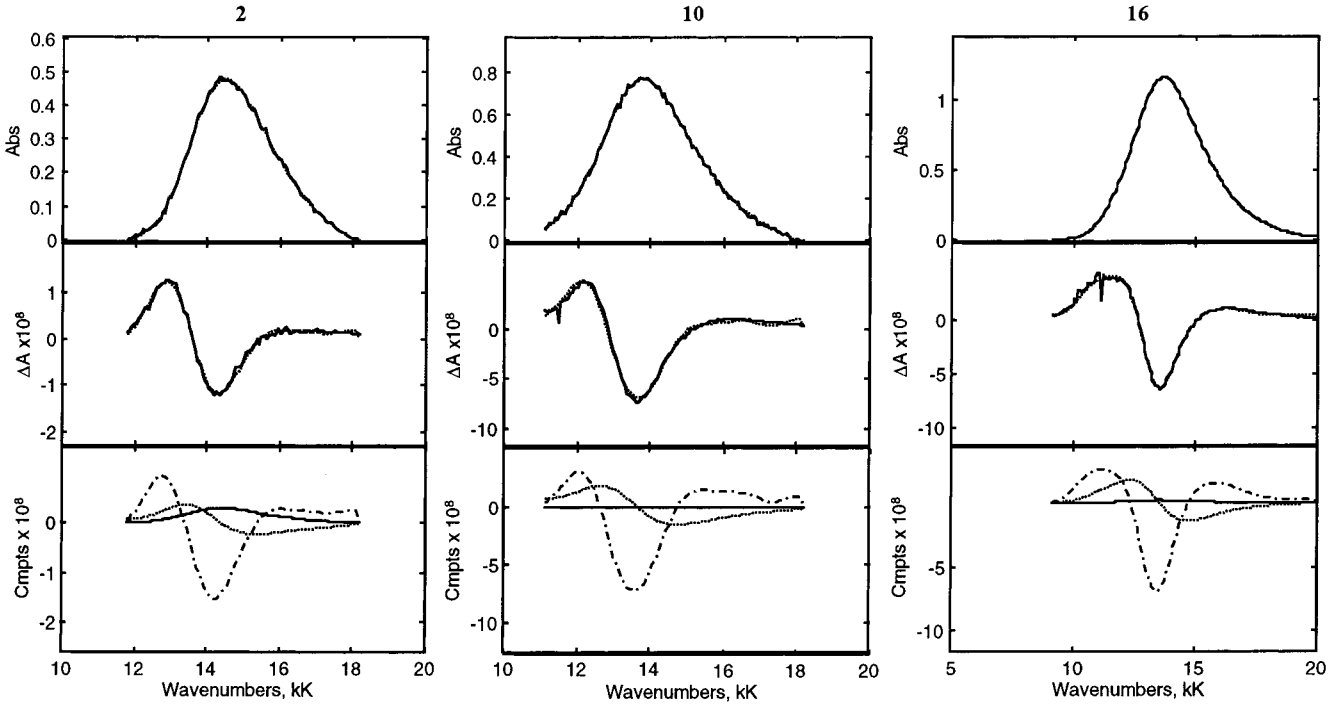

Figure 3. Electroabsorption spectra and calculated fits for the salts **2**, **10**, and **16** in external electric fields of 1.92, 3.84, and 2.39 × 10^7 V m^{-1}, respectively. Top panel, absorption spectrum; middle panel, electroabsorption spectrum, experimental (−) and fits (···) according to the Liptay equation; bottom panel, contribution of zero (−), first (···), and second (−·−) derivatives of the absorption spectrum to the calculated fits.

TABLE 1: Spectral Data and Fitting Results (eq 1[a]) for Complex Salts 1−20[b]

			λ_{max} (nm)		(eV)		(10^{-20} m^2 V^{-2})		(10^{-38} C m^2 V^{-1})		(10^{-57} C^2 m^2)		(D)	
no.	L^D	L^A	298 K	77 K	ΔE_{max}[c]	f_{os}	$f_{int}^2A_1$	$f_{int}^2A_2$	$f_{int}^2B_1$	$f_{int}^2B_2$	$f_{int}^2C_1$	$f_{int}^2C_2$	$f_{int}\lvert\Delta\mu_{12}\rvert$	$f_{int}\lvert m\cdot\Delta\mu_{12}\rvert$
1	NH_3	MeQ^+	597	645	−0.15	0.20	16.4	0.005	16.8	4.7	18.7	4.8	18.3	15.9
2	NH_3	PhQ^+	634	696	−0.17	0.22	19.3	−4.9	22.2	9.0	23.2	8.0	20.4	19.5
3	NH_3	4-$AcPhQ^+$	651	718	−0.18	0.20	44.3	13.7	24.6	9.2	28.5	10.7	22.6	22.1
4	NH_3	2,4-$DNPhQ^+$	672	731	−0.15	0.22	55.5	37.7	17.2	5.4	26.1	7.6	21.7	19.6
5	NH_3	$Mebpe^+$	604	681	−0.23	0.23	−3.4	−11.7	26.5	11.9	25.6	8.6	21.5	20.3
6	NH_3	$Phbpe^+$	641	714	−0.19	0.21	18.3	2.57	35.2	13.2	37.4	12.1	25.9	24.3
7	NH_3	$Medap^+$	590	632	−0.14	0.17	31.7	0.8	6.9	1.1	19.5	6.2	18.7	17.3
8	mim	MeQ^+	610	658	−0.15	0.22	−2.1	6.1	28.8	9.5	29.0	8.0	22.8	20.4
9	mim	PhQ^+	651	708	−0.15	0.27	8.4	−9.2	27.8	9.6	29.9	10.2	23.2	22.0
10	mim	4-$AcPhQ^+$	668	721	−0.14	0.26	15.7	14.1	27.5	10.9	27.9	10.1	22.4	21.7
11	mim	2-$PymQ^+$	715	784	−0.15	0.24	12.8	10.9	24.5	5.7	27.7	9.4	22.3	21.2
12	mim	$Mebpe^+$	616	687	−0.21	0.26	−8.7	−1.1	26.5	9.0	31.6	10.4	23.9	22.4
13	mim	$Phbpe^+$	651	741	−0.23	0.26	−5.3	−5.5	37.6	12.1	39.9	14.2	26.8	25.8
14	dmap	MeQ^+	624	667	−0.13	0.25	0.7	2.3	16.8	5.4	22.9	7.7	20.3	19.2
15	dmap	PhQ^+	663	714	−0.13	0.31	−2.8	2.4	21.5	6.5	24.8	7.6	21.1	19.4
16	dmap	4-$AcPhQ^+$	680	734	−0.13	0.30	−1.3	−5.6	34.2	11.2	40.5	14.2	27.0	25.8
17	py	2-$PymQ^+$	655	711	−0.15	0.29	−9.4	−7.8	13.8	4.4	15.2	4.2	16.5	14.7
18	py	$Mebpe^+$	577	638	−0.21	0.25	−1.82	−3.2	20.7	6.9	36.8	12.3	25.7	24.3
19	py	$Phbpe^+$	607	672	−0.20	0.26	−12.7	−9.7	27.9	9.2	41.8	13.6	27.4	25.6
20	dmabn	MeQ^+	547	571	−0.10	0.26	1.51	0.3	17.9	6.8	3.69	12.8	25.7	24.5

[a] Relationships between the parameters in eq 1 and the terms *D*-*I* defined in ref 8b are $A_1 = D/3$, $A_2 = E/30$, $B_1 = 5F$, $B_2 = G$, $C_1 = 5H$, and $C_2 = I$. [b] In butyronitrile at 77 K. [c] Shift in the MLCT band maximum energy on moving from 298 to 77 K.

c_b^2 (degree of delocalization), H_{ab} (electronic coupling matrix element), $\Delta\alpha$ (polarizability change on MLCT excitation), and β_0 (static first hyperpolarizability) values calculated from the two-state model according to eqs 7 and 9−12. Data for a number of previously measured complexes are also shown for purposes of comparison.[9b]

The μ_{12} values cover a fairly narrow range (ca. 4−7 D) and generally increase with the electron accepting strength of L^A. For the monoaryl complexes $[Ru^{II}(NH_3)_5(L^A)]^{n+}$ (n = 2 or 3), μ_{12} increases in the order L^A = py-4-NH_2 = py < pz ≈ py-4-COOH < pzH^+ < $pzMe^+$. A similar pattern is observed for the pentaammine complexes of the 4,4′-bipyridine-based L^A ligands where μ_{12} increases in the order L^A = 4,4′-bpy ≈ $Medap^+$ < MeQ^+ ≈ 4,4′-$bpyH^+$ < PhQ^+ ≈ 4-$AcPhQ^+$ = 2,4-$DNPhQ^+$. In the complexes of the other L^D ligands, μ_{12} invariably increases on replacing an *N*-methyl with a *N*-phenyl substituent, but the differences are smaller in the bpe-based complexes than in their 4,4′-bpy counterparts. Furthermore, μ_{12} is not greatly increased when a *N*-phenyl group is replaced by a more electron-deficient 4-acetylphenyl, 2,4-dinitrophenyl, or 2-pyrimidyl ring. Extension of the conjugated system by the addition of a *trans*-CH═CH bridge causes μ_{12} to change by between 0 (**2** → **6**) and +0.8 D (**8** → **12**).

Clear patterns in the variation of μ_{12} with the nature of the L^D ligand are observed, but the origins of these effects are unclear. For L^A = MeQ^+ (in **1**, **8**, **14**, and **20**), μ_{12} increases in

TABLE 2: Values of Metal-to-Ligand Distance, Transition Dipole Moment, Dipole Moment Change, Diabatic Dipole Moment Change, Electron-Transfer Distances, Degree of Delocalization, Electronic Coupling Matrix Element, Polarizability Change, and First Hyperpolarizability

no.	L^D	L^A	λ_{max} 77 K (nm)	E_{max} 77 K (10^{-19} J)	r^0 (Å)	$\lvert\mu_{12}\rvert$[a] (D)	$\lvert\Delta\mu_{12}\rvert$[b] (D)	$\Delta\mu_{ab}$[c] (D)	r_{12}[d] (Å)	r_{ab}[e] (Å)	c_b^2[f]	H_{ab}[g] (10^3 cm^{-1})	$\Delta\alpha$[h] (10^{-39} C m^2 V^{-1})	β_0[i] (10^{-49} C m^3 V^{-2})
j	NH_3	py	432	4.60	3.3	3.8	3.4	8.3	0.7	1.7	0.30	10.5	1.4	0.3
j	NH_3	pz	497	4.00	3.4	4.6	3.5	9.8	0.7	2.0	0.32	9.4	2.4	0.6
j	NH_3	pzH^+	532	3.73	3.4	5.0	≤2	≤10.2	0.2	2.1	≥0.40	≥9.2	3.0	0.2
j	NH_3	$pzMe^+$	536	3.71	3.9	5.5	≤2	≤11.2	0.2	2.3	≥0.41	≥9.2	3.7	0.2
j	NH_3	py-4-NH_2	389	5.11	3.8	3.8	5.9	9.6	1.2	2.0	0.19	10.1	1.2	0.4
j	NH_3	py-4-COOH	528	3.76	4.6	4.7	5.9	11.1	1.2	2.3	0.24	8.0	2.6	1.1
j	NH_3	4,4′-bpy	530	3.75	5.5	4.7	13	16.0	2.7	3.3	0.09	5.5	2.6	2.4
j	NH_3	4,4′-$bpyH^+$	624	3.18	5.5	5.3	17	20.0	3.5	4.2	0.07	4.2	3.9	5.5
1[k]	NH_3	MeQ^+	645	3.08	5.5	5.2	13.8	17.3	2.9	3.6	0.10	4.7	3.8	4.5
2[k]	NH_3	PhQ^+	696	2.85	7.7	5.7	15.3	19.1	3.2	4.0	0.10	4.3	5.0	6.9
3[k]	NH_3	4-$AcPhQ^+$	718	2.76	8.7	5.8	17.0	20.6	3.5	4.3	0.09	3.9	5.6	8.5
4[k]	NH_3	2,4-$DNPhQ^+$	731	2.72	8.7	5.8	16.3	20.0	3.4	4.2	0.09	4.0	3.9	8.4
5[k]	NH_3	$Mebpe^+$	681	2.92	6.7	5.5	16.2	19.6	3.4	4.1	0.09	4.1	6.0	6.5
6[k]	NH_3	$Phbpe^+$	714	2.79	8.8	5.7	19.5	22.6	4.1	4.7	0.07	3.5	8.0	9.2
7[k]	NH_3	$Medap^+$	632	3.14	5.5	4.8	14.1	17.1	2.9	3.6	0.09	4.4	1.6	3.7
8[k]	mim	MeQ^+	658	3.01	5.5	5.5	17.1	20.3	3.6	4.2	0.08	4.1	6.5	6.3
9[k]	mim	PhQ^+	708	2.80	7.7	6.2	17.4	21.4	3.6	4.5	0.09	4.1	6.3	9.6
10[k]	mim	4-$AcPhQ^+$	721	2.74	8.7	6.4	16.8	21.1	3.5	4.4	0.10	4.2	6.2	10.4
11[k]	mim	2-$PymQ^+$	784	2.53	7.7	6.4	16.8	21.1	3.5	4.4	0.10	3.9	5.6	12.0
12[k]	mim	$Mebpe^+$	687	2.88	6.7	6.3	18.0	22.0	3.7	4.6	0.09	4.2	6.0	9.5
13[k]	mim	$Phbpe^+$	741	2.68	8.8	6.5	20.2	24.0	4.2	5.0	0.08	3.6	8.5	13.1
14[k]	dmap	MeQ^+	667	2.96	5.5	6.1	15.3	19.6	3.2	4.1	0.11	4.6	3.8	7.1
15[k]	dmap	PhQ^+	714	2.77	7.7	7.1	15.9	21.3	3.3	4.4	0.13	4.6	4.9	11.6
16[k]	dmap	4-$AcPhQ^+$	734	2.71	8.7	6.8	20.3	24.4	4.2	5.1	0.08	3.8	7.7	14.4
17[k]	py	2-$PymQ^+$	711	2.79	7.7	6.5	12.4	18.0	2.6	3.7	0.15	5.1	3.1	7.5
18[k]	py	$Mebpe^+$	638	3.11	6.7	6.0	19.3	22.7	4.0	4.7	0.08	4.1	4.7	8.1
19[k]	py	$Phbpe^+$	672	2.96	8.8	6.2	20.6	24.0	4.3	5.0	0.07	3.8	6.3	10.0
20[k]	dmabn	MeQ^+	571	3.48	5.5	5.7	19.3	22.4	4.0	4.7	0.07	4.5	4.1	5.8

[a] Transition dipole moment calculated from eq 8. [b] Dipole moment change calculated from $f_{int}\lvert\Delta\mu_{12}\rvert$ using $f_{int} = 1.33$. [c] Diabatic dipole moment change calculated from eq 7. [d] Delocalized electron-transfer distance calculated from $\Delta\mu_{12}/e$. [e] Effective (localized) electron-transfer distance calculated from $\Delta\mu_{ab}/e$. [f] Degree of delocalization calculated from eq 9. [g] Electronic coupling matrix element calculated from eq 10. [h] Polarizability change calculated from eq 11. [i] First hyperpolarizability calculated from eq 12. [j] In 1:1 glycerol:water (pz = pyrazine, pzH^+ = *N*-protonated pyrazine, $pzMe^+$ = *N*-methylated pyrazine, and 4,4′-$bpyH^+$ = *N*-protonated 4,4′-bipyridine).[9b] [k] In butyronitrile, this work.

the order $L^D = NH_3$ < mim < dmabn < dmap, and a similar trend is found for $L^A = PhQ^+$ (in **2**, **9**, and **15**) or 4-$AcPhQ^+$ (in **3**, **10**, and **16**). The difference in μ_{12} between the two extremes is 1.4 D for the PhQ^+ series. For $L^A = Mebpe^+$ (in **5**, **12**, and **18**) or $Phbpe^+$ (in **6**, **13**, and **19**), μ_{12} increases in the order $L^D = NH_3$ < py < mim.

The values of $\Delta\mu_{12}$ for the pentaammine complexes generally increase as the size of L^A increases because of the addition of aryl rings and/or *trans*-CH═CH units. Similar effects are generally observed in the complexes where L^D = mim or dmap. For $L^D = NH_3$ (in **1**−**3**) or dmap (in **14**−**16**), $\Delta\mu_{12}$ increases with L^A length in the order MeQ^+ < PhQ^+ < 4-$AcPhQ^+$. However, when L^D = mim, the $\Delta\mu_{12}$ values are very similar for $L^A = MeQ^+$, PhQ^+, 4-$AcPhQ^+$ or 2-$PymQ^+$ (in **8**−**11**). The insertion of a *trans*-CH═CH bridge between the two 4,4′-bipyridinium rings in **1**, **2**, **8**, or **9** causes $\Delta\mu_{12}$ to increase by ca. 1−4 D. A similar effect of increasing $\Delta\mu_{12}$ with conjugation length is also observed in purely organic NLO chromophores.[1] The parallel between the r^0 and $\Delta\mu_{12}$ values suggests that the ligand π^* orbital is partially delocalized over multiple aryl rings. The same result is suggested by ZINDO calculations on the complexes (see below). The close similarity between the $\Delta\mu_{12}$ and $\Delta\mu_{ab}$ values of **1** and of its $Medap^+$ analogue (**7**) suggests that any torsion between the 4,4′-bipyridinium rings does not significantly reduce the delocalization of the L^A π^* orbital.

The dependence of $\Delta\mu_{12}$ on L^D is less readily explained. For $L^A = MeQ^+$ (in **1**, **8**, **14**, and **20**), $\Delta\mu_{12}$ increases in the order $L^D = NH_3$ < dmap < mim < dmabn, with a difference of 5.5 D between the two extremes. A parallel trend is found for $L^A = PhQ^+$ (in **2**, **9**, and **15**). However, when L^A = 4-$AcPhQ^+$, the $\Delta\mu_{12}$ values are very similar for $L^D = NH_3$ (in **3**) and mim (in **10**) but larger for L^D = dmap (in **16**). For $L^A = Mebpe^+$ (in **5**, **12**, and **18**) or $Phbpe^+$ (in **6**, **13**, and **19**), $\Delta\mu_{12}$ increases in the order $L^D = NH_3$ < mim < py, although the differences are only small for the $Phbpe^+$ complexes. The fact that the pentaammine complexes generally have the smallest $\Delta\mu_{12}$ values may be due to the absence of $Ru^{II} \rightarrow NH_3$ back-bonding, which allows more electron density to move toward L^A.

The $\Delta\mu_{ab}$ values for the complexes in **1**−**20** are on average 23% larger than their adiabatic counterparts. This close parallel between $\Delta\mu_{12}$ and $\Delta\mu_{ab}$ arises from the relatively modest and fairly constant μ_{12} values. The dipole moment changes can be used to calculate change-transfer distances if it is assumed that one electronic charge is transferred in an MLCT transition ($r_{12} = \Delta\mu_{12}/e$ or $r_{ab} = \Delta\mu_{ab}/e$). Values of r_{12} (the delocalized electron-transfer distance) and r_{ab} (the effective (localized) electron-transfer distance) are also included in Table 2. It can be seen that r^0 is generally about twice r_{12} and ca. 60−70% larger than r_{ab}.

The mixing between the diabatic states is reflected in c_b^2. The maximum possible value of c_b^2 is 0.5, which corresponds to essentially complete delocalization of the orbitals involved in the electronic excitation. Such a situation has been observed for the visible absorption band (λ_{max} = 538 nm at 298 K in 1:1 glycerol:water) of $[Ru^{II}(NH_3)_5(L^A)][BF_4]_3$ (L^A = *N*-methylpyrazinium), which is accordingly best described as a bonding-to-antibonding transition (this complex salt exhibits a true MLCT band at λ_{max} = 880 nm at 298 K in 1:1 glycerol:water).[9b] By contrast, the c_b^2 values for **1**−**20** are all close to 0.1 and similar to that found for $[Ru^{II}(NH_3)_5(L^A)]Cl_3$ (L^A = *N*-protonated

TABLE 3: Summary of Calculated and Experimental Values for Diabatic Dipole Moment Changes and Electron-Transfer Distances in Complexes $[Ru^{II}(NH_3)_5(L^A)]^{n+}$ ($n = 2$ or 3)

no.	L^A	N (elec)[a]	r_q[b] (10^{-2} Å)	$\Delta\mu_q$[c] (D)	$\Delta\mu_0$[d] (D)	$\Delta\mu_{ab}$ (calcd)[e] (D)	$\Delta\mu_{ab}$ (obsd) (D)
f	py	30	28	4.0	16	12	8.3
f	pz	30	24	3.5	16	13	9.8
f	pzH^+	30	25	3.6	16	13	≈10
f	$pzMe^+$	36	25	4.3	19	14	≈11
f	py-4-NH_2	36	30	5.2	18	13	9.6
f	py-4-COOH	46	23	5.1	22	17	11.1
f	4,4′-bpy	58	26	7.2	26	19	16.0
f	4,4′-$bpyH^+$	58	25	7.0	26	19	20.0
1[g]	MeQ^+	64	23	7.1	26	19	17.3
2[g]	PhQ^+	86	23	9.5	37	27	19.1
3[g]	4-$AcPhQ^+$	102	26	12.7	42	29	20.6
4[g]	2,4-$DNPhQ^+$	118	15	8.5	42	34	20.0
	2-$PymQ^+$	86	22	9.1	37	28	
5[g]	$Mebpe^+$	74	24	8.5	32	24	19.6
6[g]	$Phbpe^+$	96	23	10.6	42	31	22.6
7[g]	$Medap^+$	80	24	9.2	26	17	17.1

[a] Number of valence electrons in L^A. [b] Distance that the valence electrons move when a unit charge is placed 2 Å from the coordinating atom. [c] $r_q \times N$(elec). [d] Dipole moment change for a unit charge to move a distance r^0. [e] Calculated from $\Delta\mu_0 - \Delta\mu_q$. [f] In 1:1 glycerol:water.[9b] [g] In butyronitrile, this work.

4,4′-bipyridine).[9b] Such a limited degree of delocalization is clearly consistent with the description of the low energy absorption bands in **1**−**20** as MLCT in character. Comparison of the present values of c_b^2 and H_{ab} with those for the pentaammine complexes studied previously shows that c_b^2 tends to decrease as the L^A length increases, as would be expected. For a ligand of the size of pyridine, H_{ab} is ca. 10×10^3 cm^{-1}, whereas for the L^A ligands studied here, H_{ab} is only ca. 4×10^3 cm^{-1}, similar to that observed for protonated 4,4′-bpy. The decreases in c_b^2 and H_{ab} with length cease when L^A is longer than 4,4′-bpy. The $\Delta\alpha$ values are relatively large and generally increase in size as the length of L^A increases.

For the ruthenium ammine complexes studied previously, the difference between r_{ab} and r^0 was attributed to polarization of the ligand by the increased charge on the metal center in the excited state.[9b] This increase in charge polarizes the electrons of the ligand toward the metal and decreases the dipole moment change observed. The same effect would be expected to operate in **1**−**20**. For the largest L^A ligands, the difference between r^0 and r_{ab} is approximately 4 Å which corresponds to a difference of almost 20 D.

The results of calculations to examine the polarization effect in the pentaammine complexes are summarized in Table 3. A dummy charged atom was placed 2 Å from the coordinating atom of the ligand, and the charge center was calculated from the Mulliken orbital populations. The movement of the charge center for a unit change of charge r_q is given in Table 3. The product of r_q and the number of valence electrons in L^A gives a dipole change $\Delta\mu_q$ that is opposite to the MLCT. The diabatic dipole moment change can be estimated as the motion of one electron from the metal to the center of the ligand, $\Delta\mu_0 = r^0 \times e$, minus the polarization contribution $\Delta\mu_q$ and is included in Table 3. The plot in Figure 4 shows that, except for the longest ligands, the calculated and observed diabatic dipole moment changes are in reasonable agreement. For the complexes of the longest ligands, the calculated $\Delta\mu_{ab}$ values are too large, suggesting that the r^0 values used in these cases are too long. The ZINDO calculations (see below) also suggest that the orbital(s) that receive the MLCT electron are delocalized only over the first two aryl rings. Use of smaller r^0 values for these ligands yields better agreement.

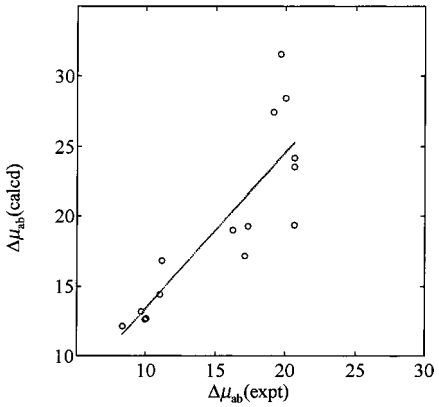

Figure 4. Plot of the calculated vs observed diabatic dipole moment changes.

ZINDO Calculations. The results of the ZINDO calculations on the pentaammine complexes are given in Table 4. The MLCT transitions for ruthenium ammine complexes are strongly solvatochromic,[3c,5a] and the models used include explicit solvent molecules around the ammine ligands. Despite these solvent molecules and/or the use of a continuum solvent cavity, the calculated E_{max} values are all too high (in several cases by a factor of almost 2) when compared with those measured in solution. By contrast, the extent of calculated vs experimental correlation for the other data is rather variable. For the previously studied complexes of monoaryl L^A ligands,[9b] the agreement is relatively poor. In particular, for the complexes with fully delocalized ground states ($L^A = pzH^+$ or $pzMe^+$), the calculated dipole moment changes are much too large and the calculated c_b^2 values are too low. However, ZINDO generally reproduces the dipole properties more accurately for the complexes of bi- or triaryl ligands. Indeed, where $L^A =$ 4-$AcPhQ^+$ (in **3**) or 2,4-$DNPhQ^+$ (in **4**), the calculated μ_{12}, $\Delta\mu_{12}$, and $\Delta\mu_{ab}$ are close ($\pm \leq 25\%$) to the experimentally determined values. Similarly good correlations are found for two out of these three quantities for $L^A =$ 4,4′-$bpyH^+$, MeQ^+ (in **1**), PhQ^+ (in **2**), $Mebpe^+$ (in **5**), or $Medap^+$ (in **7**). Of primary importance for the purposes of the present study, the calculated vs experimental agreement for β_0 is generally very poor, especially for the complexes of monoaryl ligands. However, the ZINDO static first hyperpolarizabilities are within ±25% of their electroabsorption-derived values for $L^A =$ py-4-COOH, 4,4′-bpy, 4,4′-$bpyH^+$, MeQ^+ (in **1**), or $Mebpe^+$ (in **5**).

The ZINDO calculations also show that for the MLCT transitions the angles between μ_{12} and $\Delta\mu_{12}$ are small. Analysis of the orbitals involved in these transitions indicates that systems with a third aryl ring located far from the metal center possess a high lying π-bonding orbital located on this ring. This orbital often contributes to the MLCT transition with charge transferring in a direction opposite to the metal-to-ligand direction. This contribution to the transition tends to increase the calculated coupling and decrease the dipole moment change. Thus, for $L^A = PhQ^+$, 4-$AcPhQ^+$, 2,4-$DNPhQ^+$, or $Phbpe^+$, the calculated H_{ab} (and in several cases, c_b^2) values are larger than those observed. The calculations suggest that the low lying π^* orbitals span only the first two aryl rings and that the third ring is orbitally distinct. This suggestion is in line with the trend that the observed c_b^2 and H_{ab} reach limiting values when there are two rings as in 4,4′-bpy and also with the need to use a shorter r^0 to obtain agreement between the calculated and observed $\Delta\mu_{ab}$ values.

TABLE 4: Summary of the Results of ZINDO Calculations for the MLCT Transitions of Complexes $[Ru^{II}(NH_3)_5(L^A)]^{n+}$ ($n = 2$ or 3)

no.	L^A	λ_{max} (nm)	E_{max} (10^3 cm^{-1})	μ_{12} (D)	$\Delta\mu_{12}$ (D)	$\Delta\mu_{ab}$ (D)	r_{12} (Å)	r_{ab} (Å)	c_b^2	H_{ab} (10^3 cm^{-1})	β (10^{-49} cm^3 V^{-2})	
a	py	320	32	5.0	10	14	2.0	2.9	0.15	11.3	1.4	
a	pz	319	31	4.9	10	14	2.1	2.9	0.14	10.8	1.4	
a	pzH^+	394	25	7.6	9	18	1.9	3.7	0.24	10.9	4.7	
a	$pzMe^+$	396	25	7.6	10	18	2.0	3.7	0.23	10.7	4.9	
a	py-4-NH_2	311	32	5.4	8	13	1.6	2.8	0.21	13.1	1.3	
a	py-4-COOH	320	31	4.4	9	13	1.9	2.6	0.14	10.9	1.0	
a	4,4′-bpy	317	32	6.3	8	15	1.7	3.1	0.23	13.2	1.8	
a	$4,4'\text{-bpyH}^+$	377	27	6.8	17	22	3.7	4.6	0.10	8.1	6.5	
1[b]	MeQ^+	372	27	5.8	18	21	3.8	4.5	0.08	7.2	4.7	
2[b]	PhQ^+	382	26	6.3	11	17	2.3	3.5	0.17	9.8	3.6	MLCT and $\pi-\pi^*$
3[b]	4-AcPhQ^+	386	26	5.3	17	20	3.6	4.2	0.07	6.8	4.0	MLCT and $\pi-\pi^*$
4[b]	$2,4\text{-DNPhQ}^+$	366	27	5.0	18	21	3.8	4.4	0.06	6.5	3.5	
c	2-PymQ^+	375	27	7.1	13	20	2.8	4.1	0.15	9.6	5.5	MLCT and $\pi-\pi^*$
5[b]	$Mebpe^+$	365	27	8.1	16	23	3.3	4.7	0.15	9.8	7.8	MLCT and $\pi-\pi^*$
6[b]	$Phbpe^+$	369	27	8.3	7	18	1.4	3.7	0.31	12.6	3.5	MLCT and $\pi-\pi^*$
7[b]	$Medap^+$	384	26	3.2	14	15	2.9	3.2	0.04	5.4	1.2	

[a] In 1:1 glycerol:water.[9b] [b] In butyronitrile, this work. [c] Reference 5d (λ_{max}[MLCT] = 673 nm in acetonitrile at 298 K).

In summary, these ZINDO calculations predict the dipole properties more accurately than they do the MLCT energies or first hyperpolarizabilities. Certainly, no trends in the latter quantities can be deduced from the calculations. The particularly poor correlation of β_0 between theory and experiment for the complexes of the *N*-aryl L^A ligands can be traced to the ZINDO conclusion that the *N*-aryl rings act as electron donating substituents. Hence, the predicted E_{max} values remain essentially constant and β_0 decreases upon replacement of an *N*-methyl with an *N*-aryl group. By contrast, experiments show that this structural change in L^A leads to substantial red shifts in E_{max} and accompanying increases in β_0 (see below).[5b−d] Electrochemical measurements also confirm that *N*-arylation *increases* the electron accepting abilities of the 4,4′-bipyridinium or 4-[*trans*-2-(4-pyridyl)ethenyl]pyridinium units when compared with MeQ^+ or $Mebpe^+$.[5b−d] Hence, the aryl rings actually behave as *electron withdrawing* substituents, although the relative contributions of inductive and mesomeric effects are unclear. More sophisticated ZINDO calculations have been carried out that model the solvent with a larger solvent cavity and use a Monte Carlo method to sample various solvent configurations.[20] Although these calculations reproduce the MLCT energy of $[Ru^{II}(NH_3)_5py]^{2+}$ significantly better than those reported here, it is not known if the various other parameters are in better agreement.

First Hyperpolarizabities: Trends and Comparisons between Electroabsorption and HRS Results. The electroabsorption-derived static first hyperpolarizabilities, β_0[Stark], (converted into esu) are presented in Table 5, together with the λ_{max} and β_0[HRS] values for acetonitrile solutions of **1**−**20** at 298 K.[5] The latter were derived from the application of eq 13 (*E* is the fundamental laser energy) to the β_{1064} values obtained from HRS measurements.[5]

$$\beta_{1064} = \beta_0 \frac{{E_{max}}^2}{[1 - (2E)^2({E_{max}}^2)^{-1}][(E_{max})^2 - E^2]} \qquad (13)$$

Other two-state descriptions are also available, which would change the β_0[Stark] values quoted here by a constant factor of either 0.5 or 2.[21] However, it is noteworthy that, when using eq 12, the extent of agreement between β_0[Stark] and β_0[HRS] is generally good and, in four cases, excellent ($\leq \pm 5\%$). The complexes with the smallest and the largest β_0 values are the same in both data series (in salts **7** and **16**, respectively). The poor correlations observed for **18** and **20** can be traced to the fact that the β_0[HRS] values of these compounds are underestimated because of the close proximity of their MLCT maxima to the second harmonic wavelength at 532 nm.[5d,a] Hence, the β_0[Stark] values for **18** and **20** are more reliable estimates of their actual static first hyperpolarizabilities. Importantly, the present studies confirm the very large magnitudes of β_0 in Ru^{II} penta/tetraammine complexes with pyridinium ligands. Furthermore, they also provide support for our earlier conclusion that the quadratic NLO responses of the *N*-arylpyridinium Ru^{II} chromophores are larger than those of their *N*-methyl analogues.[5b−d]

TABLE 5: First Hyperpolarizabilities Derived from Electroabsorption Spectra and Hyper-Rayleigh Scattering for Complex Salts 1−20

no.	L^D	L^A	λ_{max}[a] (nm)	β_0[Stark][b] (10^{-30} esu)	β_0[HRS][c] (10^{-30} esu)
1	NH_3	MeQ^+	590[d]	120	123[d]
2	NH_3	PhQ^+	628[d]	186	220[d]
3	NH_3	4-AcPhQ^+	654[d]	229	354[d]
4	NH_3	$2,4\text{-DNPhQ}^+$	660[d]	225	289[d]
5	NH_3	$Mebpe^+$	595[e]	175	142[e]
6	NH_3	$Phbpe^+$	628[e]	249	192[e]
7	NH_3	$Medap^+$	581[e]	98	89[e]
8	mim	MeQ^+	602[f]	170	100[f]
9	mim	PhQ^+	648[d]	258	254[d]
10	mim	4-AcPhQ^+	666[d]	279	332[d]
11	mim	2-PymQ^+	698[e]	323	336[e]
12	mim	$Mebpe^+$	604[e]	256	168[e]
13	mim	$Phbpe^+$	638[e]	352	310[e]
14	dmap	MeQ^+	614[f]	191	130[f]
15	dmap	PhQ^+	658[d]	313	260[d]
16	dmap	4-AcPhQ^+	688[d]	388	410[d]
17	py	2-PymQ^+	644[e]	200	228[e]
18	py	$Mebpe^+$	563[e]	218	78[e]
19	py	$Phbpe^+$	591[e]	269	151[e]
20	dmabn	MeQ^+	540[f]	157	14[f]

[a] Measured in acetonitrile at 298 K. [b] Static first hyperpolarizability calculated by using $\Delta\mu_{12}$ and μ_{12} values and eq 12. [c] Static first hyperpolarizability derived from 1064 nm HRS measurements and corrected by using the two-state model according to eq 13 (±15%). [d] Reference 5c. [e] Reference 5d. [f] Reference 5a.

Comparison of the data in Tables 2 and 5 is informative regarding the factors responsible for the observed differences and trends in β_0. Within the three triads with a given L^D (**1**−**3**, **8**−**10**, and **14**−**16**), the MLCT λ_{max} red shifts as the electron accepting strength of L^A increases in the order MeQ^+ <

PhQ^+ < 4-$AcPhQ^+$, as confirmed by electrochemical studies.[5b,c] β_0 increases in the same order, in keeping with principles well-established in dipolar organic chromophores.[1] As noted previously, for $L^D = NH_3$ (in **1**−**3**) or dmap (in **14**−**16**), $\Delta\mu_{12}$ clearly increases in the order MeQ^+ < PhQ^+ < 4-$AcPhQ^+$, but when L^D = mim (in **8**−**10**), no trend is found. By contrast, μ_{12} also increases on replacement of MeQ^+ with PhQ^+, but the values for the 4-$AcPhQ^+$ complexes are similar to those of their PhQ^+ counterparts. Hence, the observed increases in β_0 are generally associated with increases in both μ_{12} and $\Delta\mu_{12}$.

The 2,4-$DNPhQ^+$ and 2-$PymQ^+$ complexes in **4** and **11** possess essentially identical values of μ_{12} and $\Delta\mu_{12}$ and also similar β_0 values when compared with their 4-$AcPhQ^+$ analogues. As discussed previously,[5c] β_0 in **4** is smaller than would be expected, on the basis of the very strongly electron-withdrawing nature of a 2,4-DNPh ring. This observation is attributed to an attenuation of mesomeric coupling, arising from twisting about the $N_{pyridyl}-C_{phenyl}$ bond because of the steric effect of the *ortho*-NO_2 substituent.[5c] Also, it is clear that replacement of 4-$AcPhQ^+$ by the considerably more strongly electron-accepting ligand 2-$PymQ^+$ (cyclic voltammetric data show that coordinated 2-$PymQ^+$ is easier to reduce than 4-$AcPhQ^+$ by ca. 0.2 eV)[5d,22] is not an especially effective means to increase β_0, despite the significant red shifting of the MLCT absorption in moving from **10** to **11**.

The β_0 values for the $Medap^+$ complex in **7** are slightly smaller than those of the analogous MeQ^+ complex in **1**. Hence, it appears that fixing the coplanarity of the 4,4′-bipyridinium rings actually has a deleterious effect on β_0 (the original expectation was the reverse),[5d] which can be traced to a small blue shift in λ_{max}, together with a slight decrease in μ_{12} in moving from **1** to **7**. With a given L^A (MeQ^+, PhQ^+, or 4-$AcPhQ^+$), the λ_{max}, μ_{12}, and β_0[Stark] (but not always β_0[HRS]) values all increase in the order $L^D = NH_3$ < mim < dmap, but no accompanying trend in $\Delta\mu_{12}$ is observed (see above).

In purely organic dipolar chromophores, the extension of conjugated bridges leads to red shifting of charge-transfer bands and increases in $\Delta\mu_{12}$ and is, hence, a well-established strategy for enhancing β_0.[1] Given the relatively large experimental errors, our previous HRS studies failed to provide compelling evidence that insertion of a *trans*-CH═CH bond into the 4,4′-bipyridinium unit serves to enhance β_0 in Ru^{II} ammines.[5d] However, comparison of the β_0[Stark] values for the pairs **1**/**5**, **2**/**6**, **8**/**12**, and **9**/**13** does reveal increases of ca. 35−50% in each case, generally accompanied by small increases in μ_{12} and larger increases in $\Delta\mu_{12}$, as noted earlier.

Although the trends are the same, the *differences* in μ_{12} and β_0 between the pairs of $Mebpe^+$/$Phbpe^+$ complexes (in **5**/**6**, **12**/**13**, and **18**/**19**) are consistently smaller than those observed within the MeQ^+/PhQ^+ pairs. However, the reverse is true of the $\Delta\mu_{12}$ values; that is, these show larger increases on moving from *N*-Me to *N*-Ph in the bpe-based complexes than in their 4,4′-bpy-based counterparts. Both the HRS and electroabsorption studies clearly demonstrate that the β_0-enhancing effect of pyridyl *N*-phenylation is most significant in the 4,4′-bpy-based complexes.

Conclusions

The electroabsorption spectra of a series of salts *trans*-$[Ru^{II}(NH_3)_4(L^D)(L^A)][PF_6]_3$ (**1**−**20**; L^D = electron-rich ligand; L^A = electron-deficient pyridinium ligand) in butyronitrile at 77 K were successfully modeled to afford dipole moment changes $\Delta\mu_{12}$ for their MLCT excitations. The transition dipole moments μ_{12} cover a fairly narrow range (ca. 4−7 D) and generally increase with the electron accepting strength of L^A, most notably on replacing an *N*-methyl with a *N*-phenyl substituent. The $\Delta\mu_{12}$ values are large (ca. 14−21 D) and generally increase as the size of L^A increases because of the addition of aryl rings and/or *trans*-CH═CH units, suggesting that the L^A π^* orbital is partially delocalized over multiple rings. For a given L^A, the pentaammine complexes typically have the smallest μ_{12} and $\Delta\mu_{12}$ values.

A consideration of charge-transfer distances provides estimated diabatic dipole moment changes $\Delta\mu_{ab}$ which are in reasonable agreement with their experimentally observed counterparts, except for the complexes of the longest L^A ligands. This result suggests that the orbital(s) that receive the MLCT electron are delocalized only over the first two aryl rings. ZINDO calculations on the pentaammine complexes do not provide accurate predictions of the MLCT energies or static first hyperpolarizabilities β_0, but they can predict the dipole properties with reasonable accuracy. These calculations also indicate that the low lying π^* orbitals span only the first two aryl rings of L^A, while the third ring is orbitally distinct.

The β_0 values calculated by using μ_{12} and $\Delta\mu_{12}$ are generally in good agreement with those derived from HRS measurements on acetonitrile solutions of **1**−**20** at 298 K. HRS severely underestimates β_0 values where the MLCT maximum is close to the second harmonic wavelength (532 nm), and the electroabsorption-derived β_0 values are hence the first meaningful estimates available for salts **18** and **20**. The present studies confirm the unusually large magnitudes of β_0 in Ru^{II} penta/tetraammine complexes and also reinforce the conclusion that *N*-arylation is an effective means to enhance β_0. Both the HRS and electroabsorption data show that the latter effect is most significant in the 4,4′-bpy-based complexes. The observed increases in β_0 are generally associated with decreases in the MLCT energy and increases in both μ_{12} and $\Delta\mu_{12}$. Although the HRS results are less conclusive, the electroabsorption studies show that insertion of a *trans*-CH═CH bridge into the 4,4′-bipyridinium unit of L^A enhances β_0 by ca. 35−50%.

Acknowledgment. We thank the EPSRC for support and for provision of a studentship (to J.A.H.). This research was partially carried out at Brookhaven National Laboratory under Contract No. DE-AC02-98CH10886 with the U.S. Department of Energy and supported by its Division of Chemical Sciences, Office of Basic Energy Sciences.

References and Notes

(1) (a) *Nonlinear Optical Properties of Organic Molecules and Crystals*; Chemla, D. S., Zyss, J., Eds.; Academic Press: Orlando, FL, 1987; Vols. 1 and 2. (b) Bosshard, Ch.; Sutter, K.; Prêtre, Ph.; Hulliger, J.; Flörsheimer, M.; Kaatz, P., Günter, P. *Organic Nonlinear Optical Materials (Advances in Nonlinear Optics, Vol. 1.)*; Gordon & Breach: Amsterdam, The Netherlands, 1995. (c) *Nonlinear Optics of Organic Molecules and Polymers*; Nalwa, H. S., Miyata, S., Eds.; CRC Press: Boca Raton, FL, 1997.

(2) (a) Marder, S. R. In *Inorganic Materials*; Bruce, D. W., O'Hare, D., Eds.; Wiley: Chichester, U.K., 1992. (b) Kanis, D. R.; Ratner, M. A.; Marks, T. J. *Chem. Rev.* **1994**, *94*, 195−242. (c) Long, N. J. *Angew. Chem., Int. Ed. Engl.* **1995**, *34*, 21−38. (d) Whittall, I. R.; McDonagh, A. M.; Humphrey M. G.; Samoc, M. *Adv. Organomet. Chem.* **1998**, *42*, 291−362. (e) Heck, J.; Dabek, S.; Meyer-Friedrichsen, T.; Wong, H. *Coord. Chem. Rev.* **1999**, *190*−*192*, 1217−1254. (f) Le Bozec, H.; Renouard, T. *Eur. J. Inorg. Chem.* **2000**, 229−239. (g) Barlow, S.; Marder, S. R. *Chem. Commun.* **2000**, 1555−1562. (h) Lacroix, P. G. *Eur. J. Inorg. Chem.* **2001**, 339−348.

(3) See, for example: (a) Ford, P.; Rudd, De F. P.; Gaunder, R.; Taube, H. *J. Am. Chem. Soc.* **1968**, *90*, 1187−1194. (b) Ford, P. C.; Wink, D.; Di Benedetto, J. *Prog. Inorg. Chem.* **1983**, *30*, 213−271. (c) Curtis, J. C.; Sullivan, B. P.; Meyer, T. J. *Inorg. Chem.* **1983**, *22*, 224−236. (d) Winkler,

J. L.; Netzel, T. L.; Creutz, C.; Sutin, N. *J. Am. Chem. Soc.* **1987**, *109*, 2381−2392. (e) Reimers, J. R.; Hush, N. S. *J. Phys. Chem.* **1991**, *95*, 9773−9781. (f) Creutz, C.; Newton, M. D.; Sutin, N. *J. Photochem. Photobiol. A: Chem.* **1994**, *82*, 47−59.

(4) (a) Clays, K.; Persoons, A. *Phys. Rev. Lett.* **1991**, *66*, 2980−2983. (b) Clays, K.; Persoons, A. *Rev. Sci. Instrum.* **1992**, *63*, 3285−3289. (c) Hendrickx, E.; Clays, K.; Persoons, A. *Acc. Chem. Res.* **1998**, *31*, 675−683.

(5) (a) Coe, B. J.; Chamberlain, M. C.; Essex-Lopresti, J. P.; Gaines, S.; Jeffery, J. C.; Houbrechts, S.; Persoons, A. *Inorg. Chem.* **1997**, *36*, 3284−3292. (b) Coe, B. J.; Essex-Lopresti, J. P.; Harris, J. A.; Houbrechts S.; Persoons, A. *Chem. Commun.* **1997**, 1645−1646. (c) Coe, B. J.; Harris, J. A.; Harrington, L. J.; Jeffery, J. C.; Rees, L. H.; Houbrechts S.; Persoons, A. *Inorg. Chem.* **1998**, *37*, 3391−3399. (d) Coe, B. J.; Harris, J. A.; Asselberghs, I.; Persoons, A.; Jeffery, J. C.; Rees, L. H.; Gelbrich T.; Hursthouse, M. B. *J. Chem. Soc., Dalton Trans.* **1999**, 3617−3625.

(6) (a) Coe, B. J.; Houbrechts, S.; Asselberghs, I.; Persoons, A. *Angew. Chem., Int. Ed. Engl.* **1999**, *38*, 366−369. (b) Coe, B. J. *Chem. Eur. J.* **1999**, *5*, 2464−2471.

(7) Bublitz, G.; Boxer, S. G. *Annu. Rev. Phys. Chem.* **1997**, *48*, 213−242.

(8) (a) Oh, D. H.; Boxer, S. G. *J. Am. Chem. Soc.* **1990**, *112*, 8161−8162. (b) Oh, D. H.; Sano, M.; Boxer, S. G. *J. Am. Chem. Soc.* **1991**, *113*, 6880−6890.

(9) (a) Shin, Y. K.; Brunschwig, B. S.; Creutz, C.; Sutin, N. *J. Am. Chem. Soc.* **1995**, *117*, 8668−8669. (b) Shin, Y. K.; Brunschwig, B. S.; Creutz, C.; Sutin, N. *J. Phys. Chem.* **1996**, *100*, 8157−8169. (c) Brunschwig, B. S.; Creutz, C.; Sutin, N. *Coord. Chem. Rev.* **1998**, *177*, 61−79.

(10) (a) Vance, F. W.; Karki, L.; Reigle, J. K.; Hupp, J. T.; Ratner, M. A. *J. Phys. Chem. A* **1998**, *102*, 8320−8324. (b) Bublitz, G. U.; Laidlaw, W. M.; Denning, R. G.; Boxer, S. G. *J. Am. Chem. Soc.* **1998**, *120*, 6068−6075. (c) Vance, F. W.; Slone, R. V.; Stern, C. S.; Hupp, J. T. *Chem. Phys.* **2000**, *253*, 313−322.

(11) Vance, F. W.; Hupp, J. T. *J. Am. Chem. Soc.* **1999**, *121*, 4047−4053.

(12) Bublitz, G. U.; Ortiz, R.; Marder, S. R.; Boxer, S. G. *J. Am. Chem. Soc.* **1997**, *119*, 3365−3376.

(13) Karki, L.; Vance, F. W.; Hupp, J. T.; LeCours, S. M.; Therien, M. J. *J. Am. Chem. Soc.* **1998**, *120*, 2606−2611.

(14) Barlow, S.; Bunting, H. E.; Ringham, C.; Green, J. C.; Bublitz, G. U.; Boxer, S. G.; Perry, J. W.; Marder, S. R. *J. Am. Chem. Soc.* **1999**, *121*, 3715−3723.

(15) Coe, B. J.; Harris, J. A.; Clays, K.; Persoons, A.; Wostyn, K.; Brunschwig, B. S. *Chem. Commun.* **2001**, 1548−1549.

(16) (a) Labhart, H. *Adv. Chem. Phys.* **1967**, *13*, 179−204. (b) Liptay, W. In *Excited States*; Lim, E. C., Ed.; Academic Press: New York, 1974; Vol. 1, pp 129−229. (c) Baumann, W. In *Physical Methods of Chemistry*; Rossiter, B. W., Hamilton, J. F., Eds.; Wiley: New York, 1989; Vol. IIIB, pp 45−131. (d) Baumann, W.; Nagy, Z.; Maiti, A. K.; Reis, H.; Rodriques, S. V.; Detzer, N. In *Dynamics and Mechanism of Photoinduced Charge Transfer and Related Phenomena*; Mataga, N., Okada, T., Masuhara, H., Eds.; Elsevier: Amsterdam, 1992; pp 211−229.

(17) *MSI Cerius*^{2}, version 4.2; Molecular Simulation Inc.: San Diego, CA, 2000.

(18) (a) Rappe, A. K.; Casewit, C. J.; Colwell, K. S.; Goddard, W. A., III.; Skiff, W. M. *J. Am. Chem. Soc.* **1992**, *114*, 10024−10035. (b) Castonguay, L. A.; Rappe, A. K. *J. Am. Chem. Soc.* **1992**, *114*, 5832−5842. (c) Rappe, A. K.; Colwell, K. S. *Inorg. Chem.* **1993**, *32*, 3438−3450.

(19) Mayo, S. L.; Olafson, B. D.; Goddard, W. A., III. *J. Phys. Chem.* **1990**, *94*, 8897−8909.

(20) Pearl, G. M.; Zerner, M. C. *J. Am. Chem. Soc.* **1999**, *121*, 399−404.

(21) Willetts, A.; Rice, J. E.; Burland, D. M.; Shelton, D. P. *J. Chem. Phys.* **1992**, *97*, 7590−7599.

(22) Coe, B. J.; Beyer, T.; Jeffery, J. C.; Coles, S. J.; Gelbrich T.; Hursthouse, M. B.; Light, M. E. *J. Chem. Soc., Dalton Trans.* **2000**, 797−803.